

Testing the nature of Dark Energy with Precision Cosmological constraints

Axel de la Macorra* and Erick Almaraz†

Instituto de Física, Universidad Nacional Autónoma de México

Ciudad de México, 04510 México

(Dated: May 7, 2018)

We present a Dark Energy (DE) model with a sound derivation as a natural extension of the Standard Model of particle physics with no free parameters and an excellent fit with current cosmological data improving by 21% the Λ CDM fit of the Baryon Acoustic Oscillations (BAO) measurements, specially designed to determine the dynamics of DE. DE corresponds to the lightest bound state scalar particle ϕ with a potential $V = \Lambda_c^{4+2/3} \phi^{-2/3}$ dynamically formed at the condensation energy scale Λ_c and scale factor a_c . The value of Λ_c , the exponent $n = 2/3$, and the initial conditions of ϕ are all derived quantities. We obtain an exact constraint $a_c \Lambda_c / \text{eV} = 1.0939 \times 10^{-4}$ and a theoretical prediction $\Lambda_c = 34_{-11}^{+16}$ eV, consistent with the best fit $\Lambda_c = 44.08 \pm 0.27$ eV. We test our model constraint on $a_c \Lambda_c$ by allowing a_c and Λ_c to vary independently and remarkably our prediction has a relative difference of only 0.2% with the best fit value. Unlike a cosmological constant Λ , our DE model predicts the amount of DE and leaves detectable cosmological imprints at different times and scales at a background and perturbation level.

I. INTRODUCTION

The mysterious accelerating expansion of the Universe has been well established in the last decade by a large number of independent observational experiments to unravel the origin of Dark Energy. Among these observations we have the Cosmic Microwave Background Radiation (CMB) [1], BAO and Large Scale Structure (LSS) surveys [2–4], Type Ia Supernovae (SNIa) [5], and local H_o measurements [6]. Ambitious projects such as DESI [7], LSST [8] and Euclid [9] are scheduled to start operating in the near future. The unprecedented amount of precise cosmological data gathered in the last decade allows us to set tight constraints and discriminate DE models. These recent precision cosmological data, in particular the BAO measurements, show that our DE model is dynamically favoured over Λ CDM even though it has one less free parameter. The energy density of the Universe at present day is made of 69% DE, 26% Dark Matter (DM) while only 5% corresponds to the Standard Model (SM) particles consisting principally of photons, neutrinos and ordinary matter. Within the context of general relativity the standard model in cosmology (Λ CDM) assumes a cosmological constant Λ as DE, constant in space and time, and has an excellent agreement with the observations [1]. However, there is no understanding of the origin nor magnitude of Λ and hence of why and when the Universe accelerates [10]. This leads to two interesting theoretical (philosophical) problems in Λ CDM commonly referred to as the “naturalness” and the “coincidence” problems. The “naturalness problem” requires to fine tune the value of the energy density ρ_Λ to an incredible one part in 10^{120} at an initial epoch, usually taken as the Planck $M_{pl} = 1.9 \times 10^{19}$ GeV or the unification

$\Lambda_{\text{gut}} \simeq 10^{16}$ GeV scales (see Fig.(1c)), while the “coincidence problem” inquires why the amount of ρ_Λ is of the same order of magnitude as matter ρ_m precisely at present time. Here we show that our DE model solves both problems naturally, since it predicts the values of DE at the Λ_{gut} scale and at present time avoiding any fine tuning.

Alternative to Λ , scalar fields ϕ have been proposed as possible sources to describe DE and a wide range of models have been studied in recent years [11–16]. In particular, inverse power law (IPL) potentials $V(\phi) = M^{4+n} \phi^{-n}$ proposed by [17–19] have been widely investigated [20–22] giving an equivalent fit as Λ CDM [23]. The evolution of the energy density $\rho_\phi = \dot{\phi}^2/2 + V(\phi)$ depends on the parameters n , M and the initial conditions of ϕ . These quantities are free parameters to be adjusted by the cosmological observations or the choice of model. For example, for an IPL potential with $n = 1/2$, the evolution of the equation of state (EoS) $w = p/\rho$ close to present time can be a decreasing function from $w = -0.8$ to $w_o = -0.87$ [23] assuming V to be in the tracking regime [24]. However, for different initial conditions we can have a growing EoS from $w \simeq -1$ to $w_o \simeq -0.85$ at present time. Clearly the choice of initial conditions of ϕ is important and the current precision cosmological data, in particular the BAO measurements, allow us to constrain the dynamics of DE.

Here we present a Dark Energy model that is a natural extension of the SM (perhaps the most accurate theory in physics [25]) where the DE corresponds to the lightest meson scalar particle ϕ , a “dark pion”, dynamically formed at late times given by the scale factor a_c as a result of the non-perturbative dynamics of a hidden Dark Gauge Group (DG) [26–28]. The scalar field ϕ is not a fundamental particle but a composite particle and since its mass arises from the binding energy of the fundamental interaction of the DG, we refer to it as Bound Dark Energy (BDE). We obtain a scalar potential $V = \Lambda_c^{4+n} \phi^{-n}$ with $n = 2/3$, where the value of

* macorra@fisica.unam.mx, a.macorra@gmail.com

† ealmaraz@estudiantes.fisica.unam.mx

n , Λ_c , the initial conditions of ϕ and the onset of BDE at a_c are all derived quantities. Remarkably, our model has no free parameters and fits better the cosmological data than Λ CDM. Our DE model constraints the two parameters $a_c \Lambda_c / \text{eV} = 1.0939 \times 10^{-4}$ with best fit values $\Lambda_c = 44.02 \text{ eV}$ and $a_c = 2.48 \times 10^{-6}$. We test our model prediction on $a_c \Lambda_c$ by allowing a_c and Λ_c to vary freely and independently and we find remarkable that the relative difference between the theoretical prediction with the best-fit value is only 0.2%.

Contrary to the standard Λ CDM, where the cosmological constant has an important effect only close to present time but is negligible at early times ($\Omega_\Lambda[z > 5] < 1\%$), our DE model has a rich structure and contributes to the evolution of the universe at very different times and scales, leaving cosmological imprints allowing us to probe its validity. At high energies the DG particles are massless and amount to 43% of the energy density of the SM at the unification scale Λ_{gut} . Once the BDE is formed at a_c , the BDE density dilutes rapidly ($\rho_{\text{BDE}} \sim a^{-6}$) impacting the evolution of matter perturbations for modes k entering around a_c ($k_c = 0.925 \text{ Mpc}^{-1}$) and enhancing them up to 20% compared to Λ CDM. For $a > a_c$, BDE becomes negligible for a long period of time until recently, when it starts growing to finally dominate and accelerate the universe close to present time. The evolution of ρ_{BDE} at late times has a growing EoS from $w \simeq -1$ to $w_o = -0.93$. Our BDE model modifies the cosmological distances and structure growth at late times in a similar but distinguishable form than Λ CDM.

II. BOUND DARK ENERGY

The dark energy model presented here introduces a supersymmetric Dark Gauge Group (DG) $SU(N_c)$ with $N_c = 3$ colors and $N_f = 6$ elementary massless particles in the fundamental representation [28, 29]. The values of N_c and N_f have the same fundamental status as the gauge groups and number of families of the SM ($SU_{\text{QCD}}(N_c = 3) \times SU(N_c = 2)_L \times U_Y(N_c = 1)$ and 3 families) describing the strong (QCD), weak and electromagnetic interactions and they are input parameters not derived from a more fundamental theory. At high energies the DG particles are weakly coupled and they contribute to the total content of radiation of the Universe. However, at lower energies the strength of the DG interaction increases and the gauge coupling becomes strong at the condensation energy scale Λ_c and scale factor a_c . At this scale the fundamental fields of the DG form gauge invariant composite states, dark mesons and dark baryons, which acquire a non-perturbative mass proportional to Λ_c . This is similar to the strong QCD force, where the masses of the protons and pions are of the order of the QCD scale $\Lambda_{\text{QCD}} = 210 \pm 14 \text{ MeV}$ [25], much larger than the fundamental quarks masses, clearly showing that the mass of the hadrons is due to the strong QCD dynamics. Dark Energy corresponds to

the lightest meson scalar particle ϕ , dynamically formed due to the non-perturbative force of the DG. In the Minimal Supersymmetric Standard Model (MSSM) the gauge couplings are unified at the unification scale $\Lambda_{\text{gut}} = (1.05 \pm 0.07) 10^{16} \text{ GeV}$ with $g_{\text{gut}}^2 = 4\pi / (25.83 \pm 0.16)$ the coupling constant [30]. As a natural extension we assume that our DG is also unified with the SM gauge groups and below this scale interact with the SM only via gravity. The DG gauge coupling evolves with energy and it becomes strong at Λ_c , given by the one-loop renormalization equation [28, 29]:

$$\Lambda_c = \Lambda_{\text{gut}} e^{-8\pi^2 / (b_o g_{\text{gut}}^2)} = 34_{-11}^{+16} \text{ eV}, \quad (1)$$

where $b_o = 3N_c - N_f = 3$ is the one-loop beta function. Therefore, the condensation scale is not a free parameter of our model but a derived quantity.

At high energies ($T \gg 1 \text{ TeV}$) all particles of the SM and DG are relativistic with energy densities $\rho_x = (\pi^2/30) g_x T_x^4$ for $x = \text{SM, DG}$, where $g_{\text{SM}}^{\text{gut}} = 228.75$ and $g_{\text{DG}}^{\text{gut}} = 97.5$ are the relativistic degrees of freedom for the MSSM and the DG, respectively [28, 29]. Since the SM and DG are unified at Λ_{gut} the particles have the same temperature $T_{\text{SM}}^{\text{gut}} = T_{\text{DG}}^{\text{gut}}$ and the ratio of the energy densities is $\rho_{\text{DG}}^{\text{gut}} / \rho_{\text{SM}}^{\text{gut}} = g_{\text{DG}}^{\text{gut}} / g_{\text{SM}}^{\text{gut}} = 0.43$. Below Λ_{gut} the SM and DG particles interact only via gravity and are no longer maintained in thermal equilibrium. We can relate the temperatures using entropy conservation obtaining $T_{\text{DG}} / T_\nu = ([g_{\text{DG}}^{\text{gut}} g_{\text{SM}}] / [g_{\text{DG}} g_{\text{SM}}^{\text{gut}}])^{1/3}$ with T_ν the neutrino temperature. The number of relativistic particles of the SM varies with energy and at neutrino decoupling ($T \sim 1 \text{ MeV}$) we have $g_{\text{SM}}^{\nu \text{dec}} = 10.75$ while all DG particles remain massless for $a \leq a_c$, giving $g_{\text{DG}} = g_{\text{DG}}^{\text{gut}}$. At the phase transition a_c , which is below neutrino decoupling, we get the ratio:

$$\frac{\rho_{\text{DG}}^c}{\rho_{\text{SM}}^c} = \frac{g_{\text{DG}}^c}{g_{\text{SM}}^c} \left(\frac{4}{11} \frac{g_{\text{SM}}^{\nu \text{dec}}}{g_{\text{SM}}^{\text{gut}}} \right)^{4/3} = 0.1268, \quad (2)$$

with $\rho_{\text{SM}}^c = (\pi^2/30) g_{\text{SM}}^c T_\gamma^4$ and $g_{\text{SM}}^c = 3.384$, since at a_c only photons and neutrinos remain relativistic, and $T_\nu = (4/11)^{1/3} T_\gamma$. Clearly, the DG amounts to a non-negligible fraction of the total relativistic energy content of the early universe. Extra relativistic particles beyond the SM are usually parameterised by the model independent quantity N_{ex} given by $\rho_{\text{ex}} \equiv N_{\text{ex}} (\pi^2/30) (7/4) T_\nu^4$. From eq.(2) we obtain $N_{\text{ex}} = (4/7) g_{\text{DG}} (g_{\text{SM}}^{\nu \text{dec}} / g_{\text{SM}}^{\text{gut}})^{4/3} = 0.945$ for $a < a_c$ while $N_{\text{ex}} = 0$ for $a \geq a_c$ since at a_c all the DG particles become massive due to the strong interaction of the DG [31].

Once the condensation scale Λ_c is reached, the BDE meson fields ϕ are formed and we determine the scalar potential $V(\phi)$ using the analytical techniques studied in [26], giving an effective non-perturbative IPL potential which is stable against radiative corrections [28, 29]:

$$V = \Lambda_c^{4+2/3} \phi^{-2/3}, \quad (3)$$

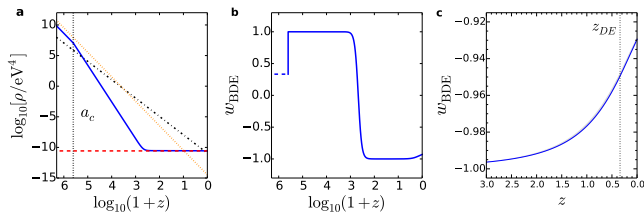


FIG. 1. (a) ρ_{BDE} (blue, solid), ρ_m (black, dash-dotted), ρ_r (orange, dotted), and ρ_Λ (red, dashed). (b) BDE EoS for $a < a_c$ (dashed) and $a \geq a_c$ (solid). (c) BDE EoS at late times. z_{DE} marks the matter-dark energy equality epoch.

where the exponent of ϕ is given by $n = -2[1 + 2/(N_c - N_f)] = -2/3$. From dimensional analysis we set the physical quantities to be proportional to the symmetry breaking scale Λ_c , giving the onset conditions of the BDE field $\phi(a_c) = \Lambda_c$, $V(a_c) = \Lambda_c^4$, $\rho_{\text{DG}}^c = 2V(a_c)/(1 - w_{\text{BDE}}^c) = 3\Lambda_c^4$, and $\dot{\phi}(a_c) = \sqrt{2\Lambda_c^4(1 + w_{\text{BDE}}^c)/(1 - w_{\text{BDE}}^c)} = 2\Lambda_c^2$, where $w_{\text{BDE}}^c = 1/3$ is the EoS at a_c and the dots stand for cosmic time derivatives. Setting $\rho_{\text{SM}}^o = \rho_{\text{SM}}^c a_c^{-4}$, $g_{\text{SM}}^o = g_{\text{SM}}^c$, $T_\gamma^o = 2.7255\text{K}$ the present temperature of photons, we get from eq.(2):

$$\frac{a_c \Lambda_c}{\text{eV}} = \left(\frac{\rho_{\text{SM}}^o g_{\text{DG}}^c}{3\text{eV}^4 g_{\text{SM}}^c} \right)^{\frac{1}{4}} \left(\frac{4 g_{\text{SM}}^{\nu\text{dec}}}{11 g_{\text{SM}}^{\text{gut}}} \right)^{\frac{1}{3}} = 1.0939 \times 10^{-4}, \quad (4)$$

which is a meaningful prediction on the two essential parameters of BDE, subject to the constraint in eq.(1).

The evolution of BDE field in a homogeneous flat universe described by the Friedmann-Lemaître-Robertson-Walker metric is completely determined by the Klein-Gordon $\ddot{\phi} + 3H\dot{\phi} + dV/d\phi = 0$ and Friedmann $H \equiv \dot{a}/a = \sqrt{8\pi G \rho_{\text{tot}}/3}$ equations. The total energy density is $\rho_{\text{tot}}(a) = \rho_{m0} a^{-3} + \rho_{r0} a^{-4} + \rho_{\text{BDE}}$ with $\rho_{\text{BDE}} = \dot{\phi}^2/2 + V(\phi)$ for BDE and ρ_{m0} , ρ_{r0} are the present day matter and radiation densities, while the redshift z is given by $a = (1+z)^{-1}$ and $a_0 = 1$ at present time. In the standard ΛCDM model ρ_{m0} and the size of the cosmological constant $\rho_\Lambda = \Lambda$ are free parameters to be determined by observations. However, in BDE for given ρ_{m0} the value of ρ_{BDE} is a predicted quantity given by the solution of the Klein-Gordon and Friedmann equations whose initial conditions are fully specified as we have just seen. Therefore, BDE not only has no free parameters but also poses one less than ΛCDM .

We study the cosmological implications of our BDE model and compare them with ΛCDM to highlight the differences. For that purpose we perform a Markov Chain Monte Carlo MCMC analysis using the `CosmoMC` [32] and `CAMB` [33] codes properly adapted to describe the full background and linear perturbation dynamics. We consider measurements of the CMB temperature anisotropies [1], BAO [2–4], and SNeIa [5] data. We vary Λ_c and determine a_c from the constriction given

by eq.(4). Table I quotes the best fits (BF) with their corresponding g.o.f. (χ^2) and the mean and 68% CL of some selected parameters. For our BDE model we obtain $\Lambda_c(\text{eV}) = 44.08 \pm 0.27$, $a_c = (2.48 \pm 0.02) \times 10^{-6}$, $\Omega_{\text{BDE}o} = 0.696 \pm 0.007$, and $w_{\text{BDE}o} = -0.929 \pm 0.001$. Notice that BDE has an excellent agreement with the cosmological measurements and a better fit than ΛCDM even though it has one less free parameter. Specifically, BDE has a significant improvement of χ_{BAO}^2 by 21%, showing that a dynamical DE is preferred. All base ΛCDM parameters [1] are consistent within 1σ with BDE. However, we find relevant tensions at more than 2σ between BDE and ΛCDM for BAO measurements and structure growth. We also test our theoretical constriction of eq.(4) by allowing a_c and Λ_c to vary freely and independently and we find remarkable that the relative difference between eq.(4) with the best-fit value $a_c \Lambda_c / \text{eV} = 1.0916 \times 10^{-4}$ is only 0.2%. The evolution of the different components for the BF is shown in (1a). Notice that at early times $\rho_\Lambda \ll \rho_r$ exposing the naturalness and coincidence problems of the ΛCDM model. Since for $a < a_c$ our model contains relativistic particles, its energy density evolves as $\rho_{\text{BDE}} \propto a^{-4}$ with non negligible energy density $\Omega_{\text{DG}}/\Omega_{\text{SM}} = 0.43(0.13)$ for $a = a_{\text{gut}}(a_c)$, respectively. However, at a_c the phase transition takes place and BDE dilutes rapidly as $\rho_{\text{BDE}} \propto a^{-6}$, taking its minimum value $\Omega_{\text{BDE}}(a \simeq 10^{-3}) \simeq 10^{-8}$ and it becomes dominant at late times with $\rho_{\text{BDE}} \approx \text{const}$ and $\Omega_{\text{BDE}} \simeq 0.69$ at present time.

In Figs.(1b) and (1c) we show the EoS of BDE and we notice that after a_c w_{BDE} leaps to 1 and remains at this value for a long period of time, then drops to -1 shortly after decoupling $z_* = 1089.98$ to finally grow to $w_{\text{BDE}o} = -0.93$ at present time. For the BF we obtain the bounds $-1 < w_{\text{BDE}} \leq -0.99, -0.95$ for $z \geq 1.8, 0.35$ while $\Omega_{\text{BDE}} \leq 1\%, 0.1\%$ for $z \geq 5.3, 12.7$. Figs.(2a) and (2b) shows the impact of Λ_c on the present density matter (Ω_m), the current expansion rate (H_o), and the BDE EoS. We see that larger values of Λ_c lead to smaller values of Ω_m and larger H_o and $w_{\text{BDE}o}$, this latter being tightly constrained.

III. OBSERVATIONAL CONSTRAINTS

A. Distances and BDE Late-Time Dynamics

The behaviour of the equation of state at recent times leads to a distinctive late-time dynamics (LTD) which has a broad impact on the cosmological observables since it modifies the amount of DE at late times. This is specially manifest in cosmological distances probed by SNIa, BAO, and CMB measurements as well as in the evolution of matter perturbations and CMB anisotropies. Distances are affected by the size and evolution of $H(z)$ which in turn depends on the amount of DE, and since $w_{\text{BDE}} > -1$ at late times, ρ_{BDE} increases as a function of z while ρ_Λ remains constant, so we expect to see dif-

TABLE I. Best fit (BF), mean and 68% parameter CL. The “base Λ CDM” parameters are given in rows 3 – 8. H_o is expressed in $\text{km}\cdot\text{s}^{-1}\text{Mpc}^{-1}$; r_{BAO} , $f\sigma_8$, and γ are evaluated at $z = 0.57$.

Parameter	BDE		Λ CDM	
	best fit	68% limits	best fit	68% limits
Λ_c (eV)	44.02	44.08 ± 0.27	—	—
$10^6 a_c$	2.48	2.48 ± 0.02	—	—
$\Omega_b h^2$	0.02252	0.02256 ± 0.00021	0.02242	0.02238 ± 0.00021
$\Omega_c h^2$	0.1173	0.1171 ± 0.0013	0.1181	0.1182 ± 0.0012
$100\theta_{\text{MC}}$	1.04106	1.04111 ± 0.00042	1.04112	1.04112 ± 0.00042
τ	0.117	0.124 ± 0.027	0.118	0.110 ± 0.027
$10^9 A_s$	2.37	2.40 ± 0.13	2.37	2.34 ± 0.12
n_s	0.9774	0.9780 ± 0.0049	0.9710	0.9701 ± 0.0048
H_o	67.68	67.80 ± 0.54	68.63	68.57 ± 0.58
$\Omega_{\text{DE}o}$	0.695	0.696 ± 0.007	0.702	0.701 ± 0.007
$w_{\text{DE}o}$	-0.9296	-0.9294 ± 0.0007	-1	-1
$\sigma_8(a_o)$	0.855	0.861 ± 0.022	0.871	0.864 ± 0.022
r_{BAO}	0.07238	0.07247 ± 0.00044	0.07230	0.07228 ± 0.00043
$f\sigma_8$	0.4883	0.4909 ± 0.0124	0.5013	0.4978 ± 0.0123
γ	0.5500	0.5499 ± 0.0001	0.5492	0.5490 ± 0.0001
z_{eq}	3342	3339 ± 29	3359	3360 ± 29
$\chi^2_{\text{BDE}} = 5.609(\text{BAO}) + 776.510(\text{CMB}) + 695.668(\text{SNeIa}) + 1.833(\text{prior})$				
$\chi^2_{\Lambda\text{CDM}} = 7.115(\text{BAO}) + 776.883(\text{CMB}) + 695.075(\text{SNeIa}) + 1.681(\text{prior})$				

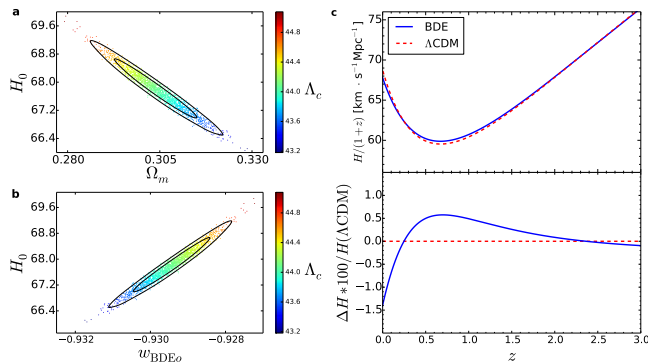


FIG. 2. (a, b) Samples in the H_o - Ω_m and H_o - $w_{\text{BDE}o}$ planes coloured by the condensation scale Λ_c (in eV). The contours mark the 68% and 95% CL. (c) Hubble expansion rate. The lower panel displays the relative difference w.r.t. Λ CDM.

ferences in BDE and Λ CDM.

Fig.(2c) shows the deviation of the expansion rate of BDE with respect to Λ CDM for the BF. We see that $H(z)$ is larger in BDE than in Λ CDM in the range $0.24 < z < 2.3$ sensitive to BAO and SNIa measurements with discrepancy of up to 0.58% at $z = 0.7$. On the other hand, H_o is smaller in BDE than in Λ CDM. This is because the accurate determination of the angular size of the sound horizon at recombination obtained from CMB measurements forces BDE and Λ CDM to have the same angular distance $D_A(z_*)$ (a difference by less than 0.05%), and since the amount of matter is roughly the same (difference less than 0.5%) the amount of ρ_{BDE} at present time must be smaller than

ρ_Λ (it is 3.7% smaller), giving a lower value of H_o^2 in BDE than in Λ CDM by 2.75%. Even though the base Λ CDM parameters are consistent within 1σ , we see in Fig.(3) a tension at more than 2σ in plots of $H_o(\Omega_m)$ vs $\Omega_c h^2$ and $H_o(\Omega_m)$ vs $r_{\text{BAO}} \equiv r_{\text{drag}}/D_V$ at $z = 0.57$, where $D_V(z) = [(1+z)^2 D_A(z)^2 z/H(z)]^{1/3}$ with $D_A(z) = (1+z)^{-1} \int_o^z dz/H(z)$ and r_{drag} the comoving sound horizon at the drag epoch [1]. These combinations of parameters allow us to probe the dynamics of the DE and is precisely in the BAO ratio r_{BAO} where we obtain a 20% reduction in $\chi^2_{\text{BAO}}(z = 0.57)$ for BDE, favouring our dynamical DE model.

The background evolution of the BDE scalar field ϕ can be well approximated by the EoS $w_{\text{fit}} = (-0.929 - 3.752z - 5.926z^2 - 4.022z^3 - 0.999z^4)/(1+z)^4$ with a relative error with w_{BDE} below 0.1% for $z < 140$ (see appendix A) and therefore the cosmological distances remain unchanged.

B. Matter Power Spectrum

The overall dynamics of the dark energy in the BDE model leaves important imprints on the evolution of matter perturbations $\delta_m \equiv \delta\rho_m/\rho_m$. Small modes ($k > k_c \equiv a_c H_c = 0.925\text{Mpc}^{-1}$) entering the horizon before a_c have distinctive features in BDE compared to standard Λ CDM as shown in Fig.(4b). Initially, the extra free streaming particles $N_{\text{ex}} = 0.945$ of the DG suppress the matter perturbations with respect to Λ CDM by nearly 1.6%, i.e., $\delta_{mi}^{\text{BDE}}/\delta_{mi}^{\Lambda\text{CDM}} \approx 0.984$. This suppression is model independent and cannot be compensated

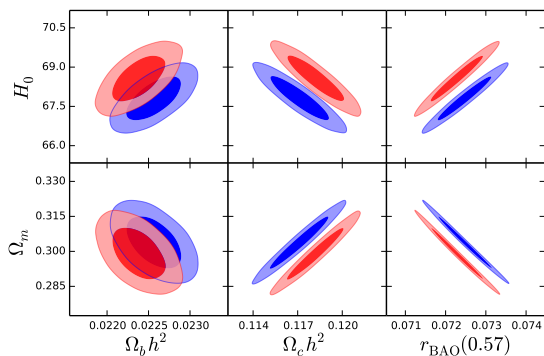


FIG. 3. 68% and 95% CL contours of H_0 and the present matter density Ω_m vs the baryon and CDM physical densities, and the BAO ratio at $z = 0.57$ for the BDE (blue) and Λ CDM (red) models.

by varying other cosmological parameters [34]. The difference of the scale factor at horizon crossing is given by $a_h^{BDE}/a_h^{\Lambda\text{CDM}} = \sqrt{1 + \rho_{DG}^c/\rho_{SM}^c} = 1.062$ (c.f. eq.(2)) allowing more time for δ_m to grow in Λ CDM and suppressing the BDE modes further. However, the change in the expansion rate after the rapid dilution of BDE makes the matter perturbations in BDE grow at a higher rate which not only compensates but reverses the initial suppression of the first two effects. The enhancement is mode dependent reaching a maximum of 7% for $k \approx 4.3\text{Mpc}^{-1}$, which agrees with the semianalytical estimation $\delta_m^{BDE}/\delta_m^{\Lambda\text{CDM}} - 1 = (\delta_{mi}^{BDE}/\delta_{mi}^{\Lambda\text{CDM}})(H_+^B/H_-^B) - 1 \simeq 5\%$ valid for modes $k > k_c$ in the range $a_{eq} > a \gg a_c$, where $H_+^B/H_-^B = \sqrt{1 + \rho_{DG}^c/\rho_{SM}^c}$ and a_{eq} is the matter-radiation equality epoch [31]. During the matter domination era δ_m grows $\propto a$ for all modes both in BDE and Λ CDM. However, at late times the LTD and the BDE field inhomogeneities suppress the growth rate of matter perturbations. The suppression factor is nearly the same for all the modes, giving a drop of $\Delta\delta_m = -0.61\%$ for the BF, with equal contributions from the LTD of the background and the DE perturbations.

The final shape of the matter power spectrum $P = 2\pi^2 P_s |\delta_m(a_o)|^2/k^3$ is a combination of the present value of $\delta_m(a_o)$ determined by the processes described above and the best fit values of n_s and A_s which define the primordial spectrum $P_s \equiv A_s(k/k_o)^{n_s-1}$. In Fig.(4b) we show the differences in the spectra for the BF. The different tilt $n_s^{BDE} > n_s^{\Lambda\text{CDM}}$ suppress the spectrum for large modes ($k < k_o = 0.05\text{Mpc}^{-1}$) and enhances it for $k > k_o$ in the BDE model. We obtain a suppression of only 1 to 3% for modes $k < k_c$ while the net effect for modes $k > k_c$ is an increase of up to 18% for BDE peaking at $k \approx 4.3\text{Mpc}^{-1}$, where the effect of the rapid dilution is maximum. This scale corresponds to a structure of radius $r = \pi/k = 0.7\text{Mpc}$ with a mean mass $M = (4\pi/3)r^3\rho_{mo} = 6.3 \times 10^{10}M_\odot$ at present time. In this regard, the enhancement in the power spectrum also increases the number density of galaxies of differ-

ent sizes $dn/dlog$. We have seen that the rapid dilution of DE strongly affects the evolution of modes in the range $0.6\text{Mpc}^{-1} < k < 9.4\text{Mpc}^{-1}$ corresponding to radiuses between $5\text{Mpc} > r > 0.3\text{Mpc}$. Using the Press-Schechter mass function [35], we find an increase of 4% in the number density $dn/dlog$ for masses between $M_i = (9 \times 10^9 - 1 \times 10^{14})M_\odot$ compared to Λ CDM. However, the final results depend on the properties and amount of DM and since modes $k > k_c$ are no longer in the linear regime a non-linear approach must be used.

The imprints on the structure formation can also be observed in the growth index γ and $f\sigma_8$, where $f \equiv d\ln(\delta_m)/d\ln(a) = \Omega_m^\gamma(a)$. While fig. (4c) shows a clear tension with Λ CDM in the $\gamma - f\sigma_8$ plane at $z = 0.57$, other parameter combinations such as $H_0 - \Omega_m^{0.5}\sigma_8$ in fig. (4d) are consistent at the 1σ level. For the BF, the differences in γ are lower than 0.3%, while the deviations in $f\sigma_8$ in fig. (4e) are up to 2.6% in the region $0.4 \leq z \leq 0.8$ with BDE suppressing $f\sigma_8$ by 2.3% (0.45%) at $z = 0(0.57)$ [31]. Future studies on redshift-space distortions will provide key evidence to settle this issue [36–41].

C. Extra Relativistic Particles

The presence of extra relativistic degrees of freedom can be constrained by current cosmological observations, so in order to be a viable model of dark energy our BDE model must be in agreement with these constraints. The amount of radiation besides photons is usually parametrized by $N_{\text{eff}} \equiv N_\nu + N_{ex}$, where $N_\nu = 3.046$ for 3 massless neutrino species. Standard analyses consider a constant N_{eff} over the whole history of the universe (e.g., [1]). These extra relativistic particles increase the expansion rate at early times modifying the amount of primordial elements formed at BBN. They affect the damping tail of the CMB spectrum [42, 43] and shift the matter-radiation epoch to a later time, leaving an additional imprint on the CMB which can be probed by the early Integrated Sachs-Wolfe effect [31, 44]. Extra relativistic particles also introduce additional anisotropic stress and modify the evolution of radiation and matter anisotropies. In our BDE model N_{ex} changes from $N_{ex} = 0.945$ for $a < a_c$ to $N_{ex} = 0$ for $a \geq a_c$, leaving then the matter-radiation equality and recombination epochs unchanged. Therefore BDE describes a cosmological scenario different than the usual constant N_{eff} . However, the extra amount of radiation in BDE during BBN increases the primordial helium Y_P and deuterium (D/H) abundances too. For the BDE model, we obtain $Y_P = 0.2587 \pm 0.0001$ (0.0003) and $D/H = (2.88 \pm 0.046(0.06)) \times 10^{-5}$ at 68% CL. Although the precise BBN abundances are still under investigation and have significant uncertainties due to the cosmological measurements and the neutron life time [45], these results are consistent with the abundances obtained by astrophysical probes [46–49] well within the 2σ level.

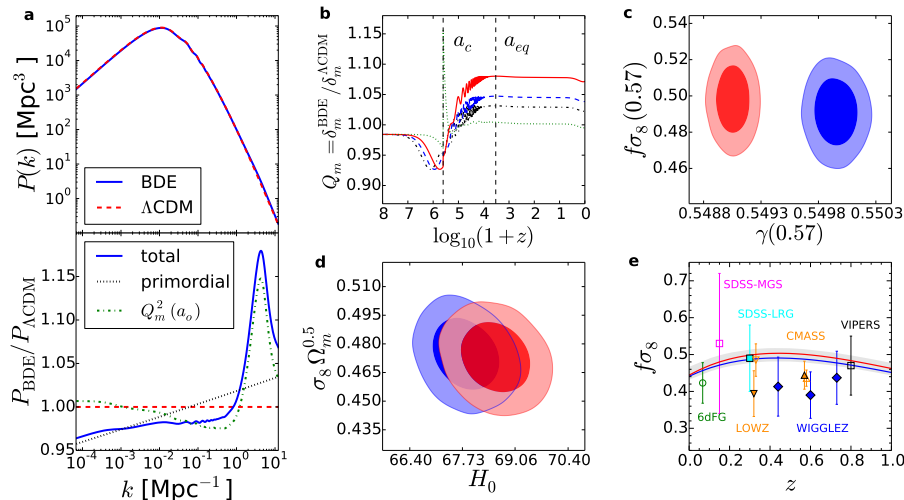


FIG. 4. (a) Matter power spectrum for the best fit. The lower panel shows the ratio w.r.t. Λ CDM of the total spectrum (blue solid), the primordial spectrum (black dotted), and $|\delta_m|^2$ at present time (green, dash-dotted). (b) Ratio of δ_m (in the newtonian gauge) for $k = 1$ (green, dotted), 4.3 (red, solid), 7 (blue, dashed), and 10Mpc^{-1} (black, dash-dotted). (c, d) 68% and 95% CL contours in the $\gamma - f\sigma_8$ at $z = 0.57$ and $H_0 - \sigma_8 \Omega_m^{0.5}$ planes for BDE (blue) and Λ CDM (red). (e) Constraints on $f\sigma_8$ for BDE (blue) and Λ CDM (red). The grey band marks the 95% CL for BDE allowed by the datasets analysed in this work. The dots are the measurements of some galaxy surveys (see references).

IV. CONCLUSIONS

We have seen that our BDE model is a natural extension of the SM of particles and without introducing any free parameters we are able to understand the current acceleration of the universe due to the dynamics of a light dark meson field. BDE also describes extra relativistic particles at high energies and a rapid dilution of its energy density at a_c . All these a priori unconnected phenomena leave distinctive measurable imprints in the universe. Our BDE model is not only predictive but it allows to understand the nature of DE.

Appendix A: Equation of state fit

Instead of solving the dynamical equation of the BDE background given by scalar field ϕ , we can estimate its evolution and cosmological effects by using an effective EoS given by the ansatz $w_{\text{fit}} = (-0.929 - 3.752z - 5.926z^2 - 4.022z^3 - 0.999z^4)/(1+z)^4$. We show in Fig.(5) the evolution of w_{fit} and compared it to w_{BDE} , obtaining an excellent fit with a relative error below 0.1% valid for $z < 140$, before $w_{\text{BDE}}(z)$ starts to grow to $w_{\text{BDE}} = 1$ (see Fig.(1b)). Our EoS ansatz accounts then for the background evolution and gives equivalent cosmological

distances and suppression factor of the matter perturbations as our BDE model. The BDE perturbations are not accounted for in our ansatz w_{fit} of the DE background, however its contributions to the linear growth of matter perturbations are smaller than 1% (see section III B) and

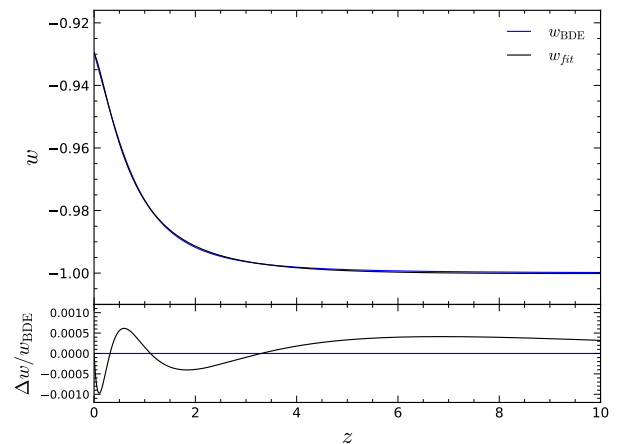


FIG. 5. We show w_{BDE} and w_{fit} and the relative difference $\Delta w = (w_{\text{fit}} - w_{\text{BDE}})/w_{\text{BDE}}$ as function of the redshift z .

they do not affect the cosmological distances.

[1] P. A. R. Ade et al., *A&A* **594**, A13 (2016).
[2] H. Gil-Marín et al., *MNRAS* **460**, 4210 (2016).

[3] A. J. Ross et al., *MNRAS* **449**, 835 (2015).
[4] F. Beutler et al., *MNRAS* **416**, 3017 (2011).

- [5] M. Betoule et al., *A&A* **568**, A22 (2014).
- [6] Adam G. Riess et al., *ApJ* **826**, 56 (2016).
- [7] <http://desi.lbl.gov/>.
- [8] <https://www.lsst.org/>.
- [9] <http://sci.esa.int/euclid/>.
- [10] J. Martin, *C. R. Physique* **13**, 566 (2012), understanding the Dark Universe.
- [11] P. A. R. Ade et al., *A&A* **594**, A14 (2016).
- [12] S. Tsujikawa, *Class. Quantum Grav.* **30**, 214003 (2013).
- [13] K. Bamba, S. Capozziello, S. Nojiri, and S. D. Odintsov, *Astrophys. Space Sci.* **342**, 155 (2012).
- [14] E. J. Copeland, M. Sami, and S. Tsujikawa, *Int. J. Mod. Phys. D* **15**, 1753 (2006).
- [15] Y. Chen, C.-Q. Geng, S. Cao, Y.-M. Huang, and Z.-H. Zhu, *JCAP* **2015**, 010 (2015).
- [16] V. Smer-Barreto and A. R. Liddle, *JCAP* **2017**, 023 (2017).
- [17] P. J. E. Peebles and B. Ratra, *ApJ* **325**, L17 (1988).
- [18] B. Ratra and P. J. E. Peebles, *Phys. Rev. D* **37**, 3406 (1988).
- [19] C. Wetterich, *Nucl. Phys. B* **302**, 668 (1988).
- [20] P.-Y. Wang, C.-W. Chen, and P. Chen, *JCAP* **2012**, 016 (2012).
- [21] A. de la Macorra and C. Stephan-Otto, *Phys. Rev. D* **65**, 083520 (2002).
- [22] P. G. Ferreira and M. Joyce, *Phys. Rev. D* **58**, 023503 (1998).
- [23] J.-M. Alimi et al., *MNRAS* **401**, 775 (2010).
- [24] P. J. Steinhardt, L. Wang, and I. Zlatev, *Phys. Rev. D* **59**, 123504 (1999).
- [25] C. Patrignani and P. D. Group, *Chinese Phys. C* **40**, 100001 (2016).
- [26] I. Affleck, M. Dine, and N. Seiberg, *Nucl. Phys. B* **256**, 557 (1985).
- [27] P. Binétruy, *Phys. Rev. D* **60**, 063502 (1999).
- [28] A. de la Macorra, *JHEP* **2003**, 033 (2003).
- [29] A. de la Macorra, *Phys. Rev. D* **72**, 043508 (2005).
- [30] U. Amaldi, W. de Boer, and H. Fürstenau, *Phys. Lett. B* **260**, 447 (1991).
- [31] E. Almaraz and A. de la Macorra, in preparation (2018).
- [32] A. Lewis and S. Bridle, *Phys. Rev. D* **66**, 103511 (2002).
- [33] A. Lewis, A. Challinor, and A. Lasenby, *ApJ* **538**, 473 (2000).
- [34] W. Hu and N. Sugiyama, *ApJ* **471**, 542 (1996).
- [35] W. H. Press and P. Schechter, *ApJ* **187**, 425 (1974).
- [36] F. Beutler et al., *MNRAS* **423**, 3430 (2012).
- [37] C. Howlett, A. J. Ross, L. Samushia, W. J. Percival, and M. Manera, *MNRAS* **449**, 848 (2015).
- [38] A. Oka, S. Saito, T. Nishimichi, A. Taruya, and K. Yamamoto, *MNRAS* **439**, 2515 (2014).
- [39] H. Gil-Marín et al., *MNRAS* **460**, 4188 (2016).
- [40] C. Blake et al., *MNRAS* **425**, 405 (2012).
- [41] S. de la Torre et al., *A&A* **557**, A54 (2013).
- [42] W. Hu and M. White, *ApJ* **479**, 568 (1997).
- [43] Z. Hou, R. Keisler, L. Knox, M. Millea, and C. Reichardt, *Phys. Rev. D* **87**, 083008 (2013).
- [44] G. Cabass et al., *Phys. Rev. D* **92**, 063534 (2015).
- [45] R. H. Cyburt, B. D. Fields, K. A. Olive, and T.-H. Yeh, *Rev. Mod. Phys.* **88**, 015004 (2016).
- [46] E. Aver, K. A. Olive, R. Porter, and E. D. Skillman, *JCAP* **2013**, 017 (2013).
- [47] Y. I. Izotov, T. X. Thuan, and N. G. Guseva, *MNRAS* **445**, 778 (2014).
- [48] F. Iocco, G. Mangano, G. Miele, O. Pisanti, and P. D. Serpico, *Phys. Rep.* **472**, 1 (2009).
- [49] S. Riemer-Sørensen et al., *MNRAS* **447**, 2925 (2015).